

# 江南造山带西段桂北龙胜地区金车辉长岩矿物 化学研究及其地质意义

寇彩化, 刘燕学, 李廷栋, 丁孝忠, 张 恒

(中国地质科学院 地质研究所, 北京 100037)

**摘要:** 桂北龙胜地区位于江南造山带西段, 本文利用电子探针对桂北龙胜地区金车辉长岩单斜辉石和斜长石进行了详细的矿物学和矿物化学研究, 研究表明单斜辉石的成分为  $W_{0.27\sim0.28}E_{n47\sim57}F_{s15\sim22}$ , 属于普通辉石, 斜长石的成分为  $A_{n1.35\sim9.05}Ab_{90.34\sim97.45}Or_{0.36\sim1.05}$ , 为钠长石。单斜辉石温压估算结果显示, 其形成温度为  $1250\sim1350^{\circ}\text{C}$ , 该温度基本与软流圈地幔温度( $1280\sim1350^{\circ}\text{C}$ )相当, 其形成压力为  $1.31\sim2.25 \text{ GPa}$ , 对应深度为  $43.2\sim74.3 \text{ km}$ 。单斜辉石成分特征指示金车辉长岩为板内拉斑玄武岩, 结合区域地质特征, 推测金车辉长岩是裂谷构造背景下软流圈地幔物质上涌并发生减压熔融的产物。

**关键词:** 金车辉长岩; 单斜辉石和斜长石; 拉斑玄武岩浆; 温压估算; 软流圈上涌; 裂谷作用

中图分类号: P588.12<sup>+4</sup>

文献标识码: A

文章编号: 1000-6524(2017)01-0020-16

## Mineralogy and mineral chemistry of the Jinche gabbro in the Longsheng area of northern Guangxi in the western segment of the Jiangnan Orogen and its geological significance

KOU Cai-hua, LIU Yan-xue, LI Ting-dong, DING Xiao-zhong and ZHANG Heng

(Institute of Geology, Chinese Academy of Geological Sciences, Beijing 100037, China)

**Abstract:** The Longsheng area in northern Guangxi lies in the western segment of the Jiangnan Orogen. In this paper, the authors determined the chemical compositions of the clinopyroxene and plagioclase in the Jinche gabbro by electron microprobe analysis. It turns out that the clinopyroxene is augite with  $W_{0.27\sim0.28}E_{n47\sim57}F_{s15\sim22}$ , and the plagioclase is albite with  $A_{n1.35\sim9.05}Ab_{90.34\sim97.45}Or_{0.36\sim1.05}$  in composition. The crystallization temperature and pressure of clinopyroxene were estimated by the clinopyroxene-melt equilibrium and clinopyroxene isotherm, which yielded crystallization temperature, pressures and corresponding formation depth of  $1250\sim1350^{\circ}\text{C}$ ,  $1.31\sim2.25 \text{ GPa}$  and  $43.2\sim74.3 \text{ km}$ , respectively. The temperature is consistent with that of the asthenosphere lithospheric mantle ( $1280\sim1350^{\circ}\text{C}$ ), and under that depth, the decompression melting of the asthenosphere lithospheric mantle can occur. Therefore, it is inferred that the Jinche gabbro might have originated from the asthenosphere lithospheric mantle. In addition, the chemical composition of the clinopyroxene indicates that the Jinche gabbro belongs to the tholeiitic series formed in an intraplate tectonic setting. In conclusion, the authors hold that the Jinche gabbro was formed by partial melting of the upwelling asthenosphere mantle due to rifting.

收稿日期: 2016-07-06; 接受日期: 2016-12-08

基金项目: 中国地质调查项目(1212011120115, 1212011120117); 国家自然科学基金(41402052); 中国地质科学院地质研究所中央级公益性科研院所基本科研业务专项(J1602)

作者简介: 寇彩化(1985- ), 女, 博士, 主要从事岩石地球化学研究, E-mail: caihuakou@163.com。

**Key words:** Jinche gabbro; clinopyroxene and plagioclase; tholeiitic basalt series; estimating the temperature and pressure; upwelling asthenosphere; rifting

**Fund support:** Project of China geological Survey(1212011120115, 1212011120117); Natural Science Foundation of China(41402052); Research Grant from Institute of Geology, Chinese Academy of Geological Sciences (J1602)

江南造山带是扬子与华夏板块历经洋壳俯冲、弧-陆碰撞以及陆-陆碰撞等多期构造运动的产物(夏斌, 1984; 郭令智等, 1996; Li, 1999; Zhao and Cawood, 1999; Li X H *et al.*, 2003, 2009, 2010; Li Z X *et al.*, 2003; Wu *et al.*, 2006; Wang *et al.*, 2008, 2014; Zheng *et al.*, 2008; Zhang *et al.*, 2008; Zhou *et al.*, 2009; Faure *et al.*, 2009; Shu *et al.*, 2011)。江南造山带西段构造岩浆活动非常复杂,一直以来是学界研究的热点及重点地区,并取得了一系列新的研究进展,但前人研究重点探讨的是江南造山带西段1 100~770 Ma期间的岩浆岩成因和构造演化机制(Zhou *et al.*, 2007; Wang *et al.*, 2008; Li *et al.*, 2010),对之后,尤其是约730~700 Ma期间江南造山带西段构造-岩浆事件研究较为薄弱,目前见诸报道的仅有湖南中部高桥地区的震旦纪玄武岩(王孝春等, 2003)和湖南西部地区形成于约700 Ma时期的超基性岩石(寇彩化等, 2016, 2017),这限制了对江南造山带西段新元古代构造演化的完整认识。

基性-超基性侵入岩的化学成分可以反映深部地幔的物理化学状态和物质组成,被视为“深部地幔的探针”,因而可为壳幔相互作用、岩浆的起源和演化,以及该地区的构造背景提供重要约束。单斜辉石是基性-超基性岩中最为常见的造岩矿物之一,其成分和结构记录了岩浆形成及演化过程中的物理化学条件等重要信息(Streck, 2008),同时单斜辉石的化学成分与其形成的构造环境密切相关(Nisbet and Pearce, 1977)。近期,作者对位于江南造山带西段桂北龙胜县附近的金车辉长岩(形成于730 Ma左右,作者未发表数据)开展了系统矿物学及矿物化学分析,旨在探讨其母岩浆性质及其形成的物理化学条件,并为其源区特征和地球动力学背景提供有利约束。

## 1 地质背景

以江绍断裂为界,华南地区被划分为扬子板块

和华夏板块两个构造单元(图1)。扬子板块出露的最古老岩石单元为崆岭群杂岩( $\sim 3.2 \sim 2.0$  Ga)(Gao *et al.*, 1999),华夏板块最古老的岩石为浙东南闽西北地区的八都群(Yu *et al.*, 2009)。扬子板块与华夏板块在新元古代时期( $1.0 \sim 0.8$  Ga)历经洋壳俯冲、弧-陆碰撞以及陆-陆碰撞等构造运动(即“四堡运动”),古华南洋闭合,形成了江南造山带(夏斌, 1984; Li *et al.*, 1995; 郭令智等, 1996; 葛文春等, 2001; 胡受奚等, 2006; 薛怀民等, 2010; Shu *et al.*, 2011; 舒良树, 2012; Zhong *et al.*, 2016)(图1)。江南造山带呈 NEE 方向展布,西起黔东、桂北,经湘西北、赣西北、赣东北,东至皖南、浙西,长约1 500 km、宽约200 km,面积约30万平方公里(郭令智等, 1980, 1996)。造山带东段主要位于赣东北、皖南、浙西、浙东北等地区,西段位于桂北和湖南以及贵州等地区(Yao *et al.*, 2014)(图1)。

江南造山带西段桂北地区出露的最古老地层为中元古界四堡群,其次为角度不整合于其上的上元古界丹洲群。其中,四堡群为一套浅灰-浅灰绿色浅变质细粒碎屑岩、粘土岩,局部夹基性-中酸性火山岩,其中的斑脱岩 SHRIMP 锆石 U-Pb 年龄为  $822 \pm 10$  Ma(高林志等, 2011);丹洲群变质沉积岩系变质程度为低绿片岩相,由下部的合桐组和上部的拱洞组组成(图2),其岩性主要为浅变质砂砾岩、长石石英砂岩、板岩及凝灰岩,局部夹基性-中酸性火山岩,高林志等(2011)获得其下部斑脱岩 SHRIMP 锆石 U-Pb 年龄为 802 Ma。本区还出露有震旦系、寒武系和泥盆系地层(图2)。江南造山带西段构造岩浆活动复杂,中酸性和基性-超基性岩浆岩均较为发育,且大都形成于850~700 Ma之间(Li, 1999; Yan *et al.*, 2004; Zhou *et al.*, 2004, 2007, 2009; Yao *et al.*, 2013, 2014)。其中,酸性岩主要以 S 型花岗岩为主,如  $819 \pm 9$  Ma 的四堡花岗岩和  $824 \pm 4$  Ma 的三防花岗岩体等(Li, 1999; Li Z X *et al.*, 1999, 2003; Li X H *et al.*, 2003, 2010);基性-超基性岩石在江南造山带西段湘西-桂北地方均有出露,主要以岩脉岩墙形式产出,如震旦纪湖南中部高桥玄武

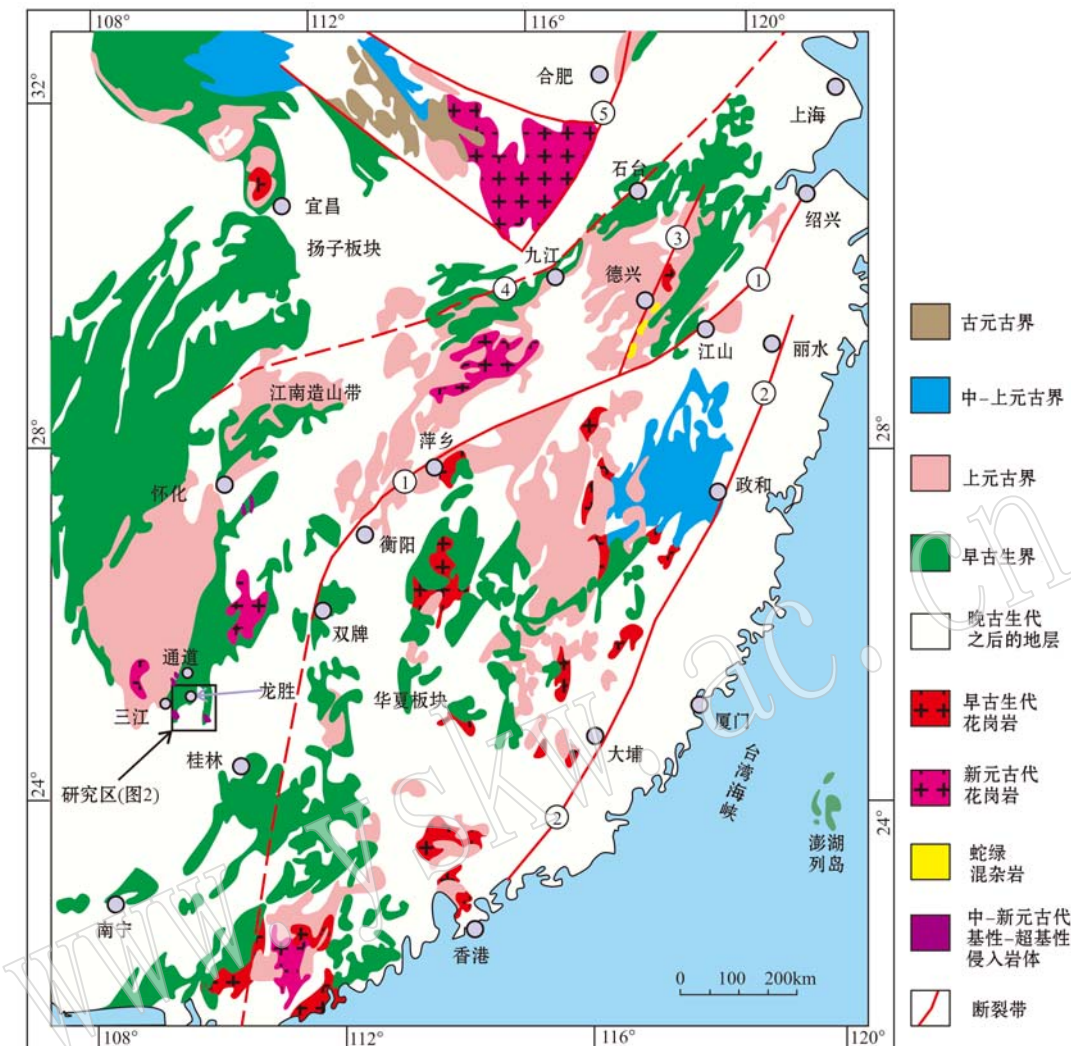


图1 江南造山带地质简图(据 Yao et al., 2014)

Fig. 1 Geological sketch map of the Jiangnan Orogen (after Yao et al., 2014)

- ①—绍兴-江山-萍乡-双牌断裂; ②—政和-大埔断裂; ③—赣东北断裂; ④—九江-石台断裂; ⑤—郯庐断裂  
 ①—Shaoxing-Jiangshan-Pingxiang-Shuangpai fault; ②—Zhenghe-Dapu fault; ③—Northeast Jiangxi fault; ④—Jiujiang-Shitai fault;  
 ⑤—Tanlu fault

岩(王孝磊等, 2003),形成于约 700 Ma 湘西通道长界橄榄辉石岩(寇彩化等, 2016)、760 Ma 的桂北龙胜辉长岩(葛文春等, 2001)、768 Ma 的湘西古丈辉绿岩(周继彬, 2006)、825 Ma 的桂北元宝山地区的超基性岩石(周继彬, 2006)以及 830 Ma 的湘西隘口辉橄岩(张春红等, 2009)等。

桂北龙胜地区分布数个基性-超基性岩体,在龙胜县附近的金车村和花桥村等地均有分布,大部分岩体呈浑圆状或者不规则状,出露面积较小,一般只有几百平方米,最大的约 0.1 km<sup>2</sup>。本次分析样品采于其中较大的金车岩体(图 3a, 3b),该岩体面积约为

0.08 km<sup>2</sup>,其岩相分带不明显,岩体呈脉状侵入于上元古界丹洲群中(图 2, 3a, 3b),其围岩为上元古界丹洲群变质沉积岩系。金车辉长岩岩性为辉长岩,手标本呈灰绿色,发育轻度蚀变,但整体比较新鲜(图 3c, 3d),作者获得该岩体的侵入年龄为 730 Ma(作者未发表数据)。

## 2 岩相学特征

金车辉长岩具有粒状结构,主要造岩矿物为单斜辉石和斜长石,其中辉石约占 65%,长石约占 30%。

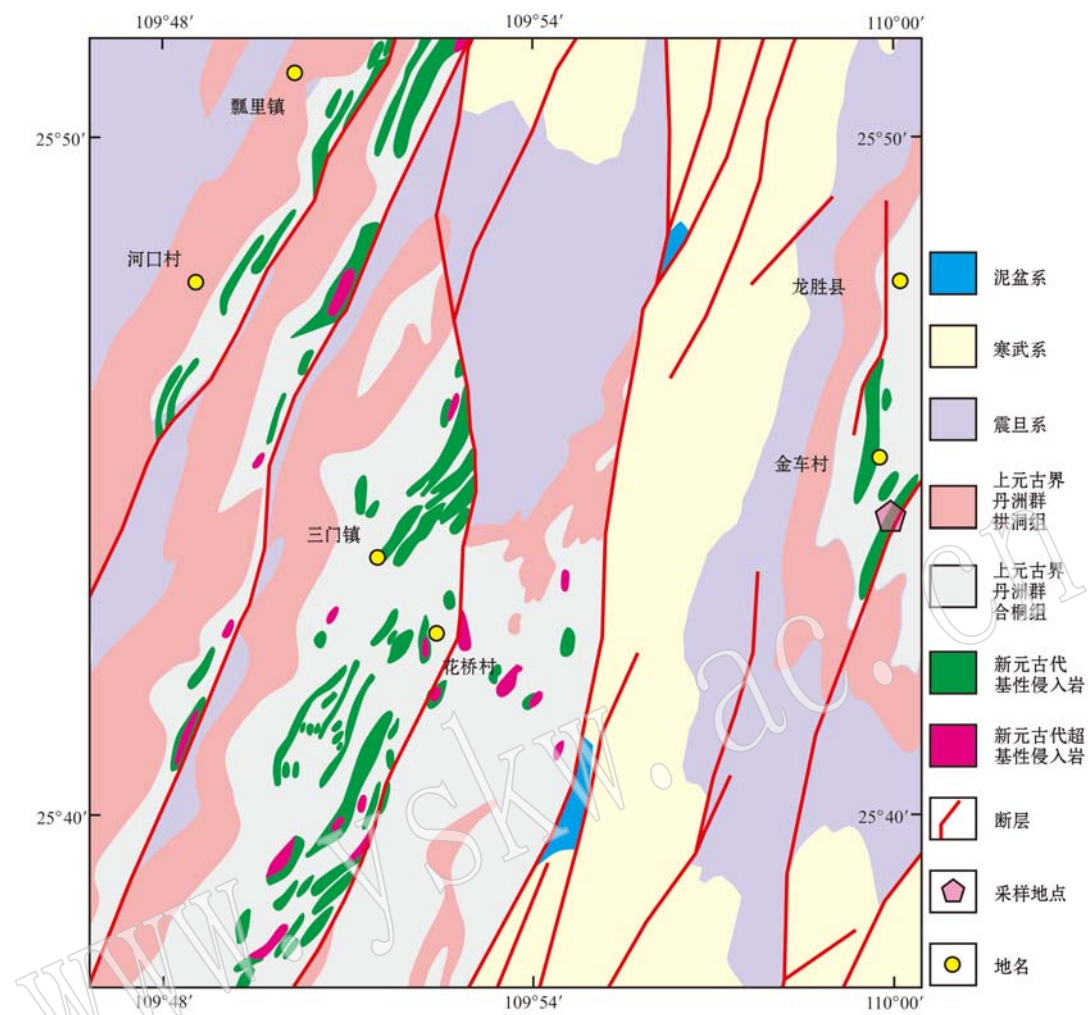


图 2 桂北龙胜地区基性-超基性岩地质图(据 1:20 万三江幅<sup>①</sup>和溆浦幅<sup>②</sup>)

Fig. 2 Sketch geological map of the mafic-ultramafic rocks from Longsheng area in north Guangxi (after 1:200 000 Geological Map of Sanjiang Sheet<sup>①</sup> and Xupu Sheet<sup>②</sup>)

单斜辉石颗粒粒径约为 0.4~5 mm, 呈自形-半自形状(图 4a, 4b, 4d, 4e)、六边形(图 4c, 4f)和板柱状(图 4g), 未见辉石环带, 镜下干涉色较高, 局部因蚀变而呈灰白色干涉色(图 4d, 4h)。斜长石颗粒粒径约为 0.3~2 mm, 多呈半自形板状, 干涉色一级灰白(图 4c, 4d, 4e, 4g, 4h, 4i), 副矿物主要为钛铁氧化物(如尖晶石)、锆石、榍石以及磷灰石等。金车辉长岩中还有一些蚀变矿物如石英(图 4h)、绿帘石(图 4d, 4i)和绿泥石(图 4g)。

### 3 样品分析方法及矿物化学特征

桂北龙胜地区金车辉长岩单斜辉石和斜长石电子探针分析在中国地质科学院地质研究所完成, 测试仪器为 JXA-8100 型电子探针仪, 加速电压 15 kV、电流 10 nA, 束斑 3  $\mu\text{m}$ , 测试误差<2% (质量分数)。单斜辉石和斜长石主量元素分析结果和以 6 个氧原子为单位计算单斜辉石和斜长石的阳离子数

<sup>①</sup> 广西壮族自治区地质局区域地质测量队, 1966. 广西壮族自治区 1:20 万三江幅地质图. 桂林: 广西壮族自治区地质局区域地质测量队.

<sup>②</sup> 湖南省革命委员会地质局区域地质测量队, 1972. 湖南省 1:20 万溆浦幅地质图. 长沙: 湖南省革命委员会地质局区域地质测量队.

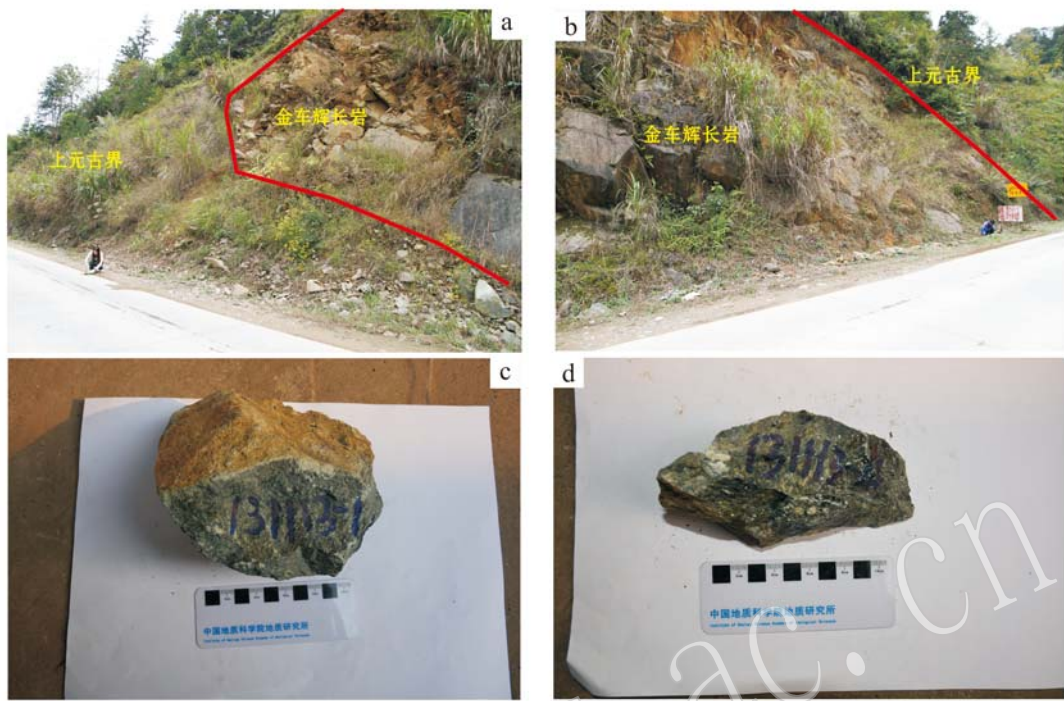


图3 金车辉长岩野外产出(a, b)和手标本(c, d)

Fig. 3 The Jinche gabbro that intruded into the Sinian lithologic sequence (a, b) and hand specimen of the Jinche gabbro (c, d)

目见表1和表2。

### 3.1 单斜辉石矿物化学特征

由表1可知,金车辉长岩单斜辉石成分变化较小,根据Morimoto等(1988)提出的辉石分类命名方案,金车辉长岩单斜辉石均属Ca-Mg-Fe辉石族(图5),其成分为 $Wo_{27\sim28}En_{47\sim57}Fs_{15\sim22}$ ,属于普通辉石(图6)。单斜辉石Mg<sup>#</sup>较高,介于68.97~78.58(平均为74),Cr<sup>#</sup>较低,为0~13.75(平均值3.5),Ca/(Ca+Mg+Fe)(Fe=Mn+Fe<sup>2+</sup>+Fe<sup>3+</sup>)也较低,为0.27~0.29,表明金车辉长岩具有低钙的特征,与其低CaO(12.18%~13.34%)一致。另外,单斜辉石大都具有较低FeO(8.54%~12.61%)、Al<sub>2</sub>O<sub>3</sub>(0.72%~3.15%)、Na<sub>2</sub>O(0.07%~0.69%)和TiO<sub>2</sub>(0~0.28%)的特征。对比而言,本次研究的金车辉长岩与邻近的湘西通道地区长界橄榄辉石岩的单斜辉石具有相似的矿物学和矿物化学特征(寇彩化等,2017),二者均具有较高Mg<sup>#</sup>、较低Cr<sup>#</sup>以及低Al<sub>2</sub>O<sub>3</sub>、低Na<sub>2</sub>O和低TiO<sub>2</sub>的特征。在单斜辉石主要氧化物相关图解(图7)上,Mg<sup>#</sup>与Al<sub>2</sub>O<sub>3</sub>和FeO呈较好的负相关性,与SiO<sub>2</sub>呈较好的正相关,但与其他氧化物(如CaO)相关性不明显。

### 3.2 斜长石矿物化学特征

由表2可知,金车岩体斜长石成分变化较小,其

An=1.35~9.05,Ab=90.34~98.06,Or=0.36~1.05,总体具有高SiO<sub>2</sub>(65.78%~68.35%)、Al<sub>2</sub>O<sub>3</sub>(19.45%~20.76%)和Na<sub>2</sub>O(9.87%~11.44%)以及低CaO(0.29%~1.89%)的特征。在斜长石分类图解An-Ab-Or中(图8),均落入钠长石范围内,指示金车辉长岩中的斜长石已经被蚀变为钠长石。

## 4 讨论

### 4.1 岩浆系列

单斜辉石的成分取决于母岩浆的成分与结晶环境(邱家壤等,1996; Le Bas, 1962; Leterrier *et al.*, 1982; Sun and Bertand, 1991; Seyler and Bonatti, 1994; 孙传敏, 1994),因此,其成分能够较好地反映其母岩浆成分特征。如图9所示,单斜辉石高SiO<sub>2</sub>而低Al<sub>2</sub>O<sub>3</sub>和TiO<sub>2</sub>的特征指示其寄主岩石的母岩浆为亚碱性系列,在Al<sub>2</sub>O<sub>3</sub>-Na<sub>2</sub>O-TiO<sub>2</sub>和SiO<sub>2</sub>-Na<sub>2</sub>O-TiO<sub>2</sub>图解中(图10),单斜辉石均落入拉斑玄武岩系列,与单斜辉石成分图解(图6)结果一致。另外,单斜辉石相关图解显示(图7),随着岩浆的演化,岩浆成分由富镁向富铁的方向演化,也指示其岩浆为拉斑玄武岩系列。

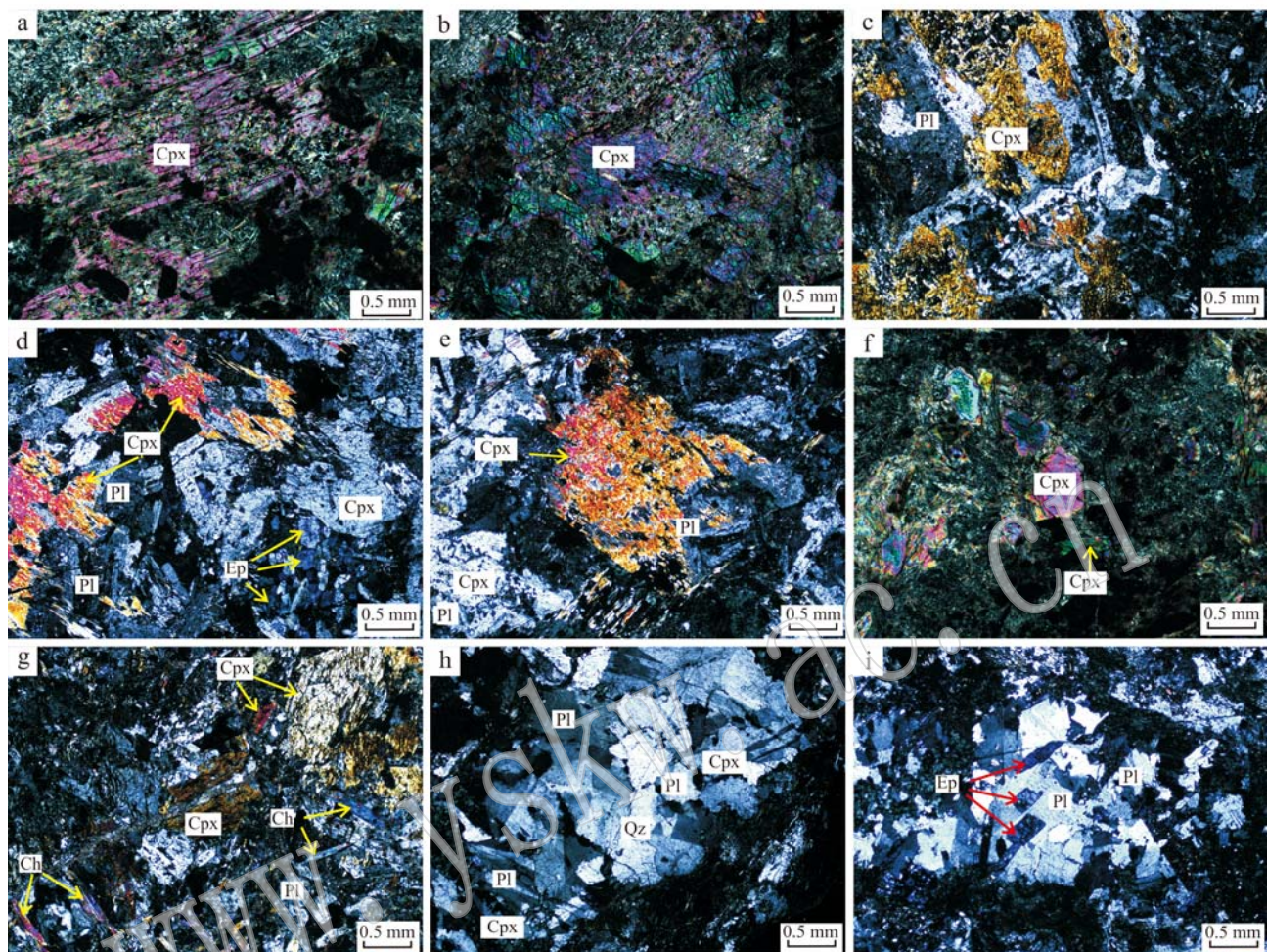


图4 金车辉长岩镜下特征(正交偏光)

Fig. 4 Photomicrograph showing major minerals and texture of the Jinche gabbro (crossed nicols)

Cpx—单斜辉石; Pl—斜长石; Qz—石英; Ep—绿帘石; Ch—绿泥石

Cpx—clinopyroxene; Pl—plagioclase; Qz—quartz; Ep—epidote; Ch—chlorite

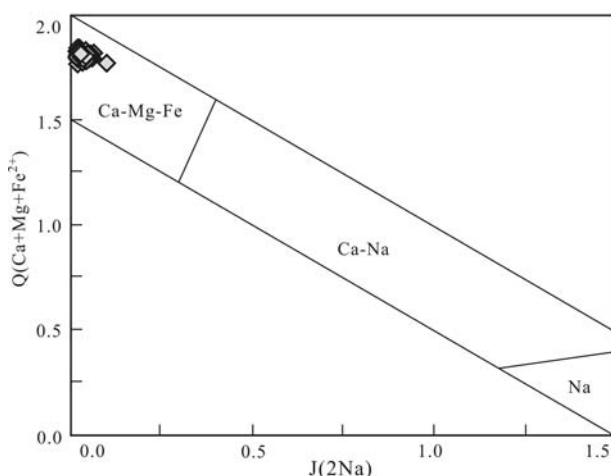


图5 单斜辉石系列Q-J图解(底图据 Morimoto et al., 1988)

Fig. 5 Diagram of Q-J series for clinopyroxenes (after Morimoto et al., 1988)

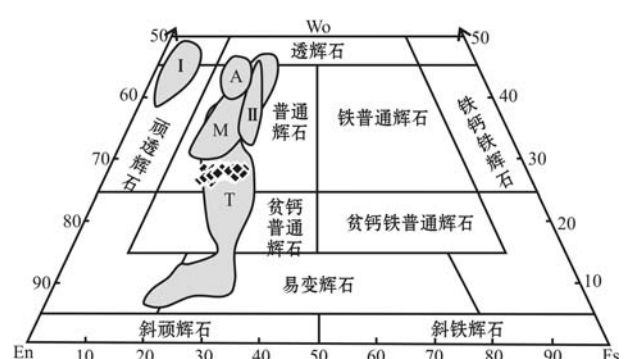


图6 单斜辉石分类图解(底图据邱家骥等, 1996)

Fig. 6 Diagram of classification for clinopyroxenes  
(after Qiu Jiaxiang et al., 1996)I—I型包体; II—II型包体; M—巨晶; A—碱性玄武岩  
系列; T—拉斑玄武岩系列I—I-type inclusion; II—II-type inclusion; M—megacryst;  
A—alkali basalt series; T—tholeiitic basalt series





续表 1-2

Continued Table 1-2

样号	JC13-3	JC13-3	JC13-6								
SiO <sub>2</sub>	55.00	53.72	53.75	53.84	52.78	53.41	53.17	53.05	54.07	53.81	53.24
TiO <sub>2</sub>	0.06	0.03	0.01	0.04	0.02	0.03	0.00	0.11	0.00	0.05	0.01
Al <sub>2</sub> O <sub>3</sub>	1.33	2.35	2.23	1.96	3.15	2.34	2.26	2.31	1.80	2.04	2.30
Cr <sub>2</sub> O <sub>3</sub>	0.00	0.00	0.12	0.10	0.36	0.35	0.05	0.01	0.00	0.00	0.15
FeO	10.31	10.51	11.82	11.88	12.38	11.53	12.61	12.25	11.35	11.58	11.90
MnO	0.17	0.19	0.28	0.21	0.23	0.19	0.25	0.24	0.22	0.25	0.23
MgO	17.66	16.84	16.47	16.43	15.63	16.33	16.04	16.50	16.84	16.63	16.11
CaO	12.91	12.97	12.54	12.38	12.86	12.75	12.59	12.58	12.99	13.18	12.66
Na <sub>2</sub> O	0.12	0.28	0.26	0.15	0.29	0.20	0.14	0.12	0.18	0.14	0.25
K <sub>2</sub> O	0.04	0.11	0.07	0.04	0.10	0.09	0.07	0.08	0.08	0.14	0.10
NiO	0.04	0.03	0.01	0.02	0.06	0.00	0.00	0.00	0.05	0.00	0.03
Total	97.63	97.03	97.55	97.05	97.86	97.21	97.19	97.25	97.58	97.81	97.04
Si	2.043 3	2.015 5	2.015 5	2.027 0	1.984 8	2.009 6	2.009 8	2.001 2	2.024 4	2.013 9	2.011 0
Al <sup>IV</sup>	0.000 0	0.000 0	0.000 0	0.000 0	0.015 2	0.000 0	0.000 0	0.000 0	0.000 0	0.000 0	0.000 0
Al <sup>VI</sup>	0.058 1	0.103 7	0.098 5	0.087 1	0.124 4	0.103 6	0.100 8	0.102 8	0.079 5	0.089 8	0.102 3
Ti	0.001 7	0.000 8	0.000 3	0.001 1	0.000 5	0.000 9	0.000 0	0.003 1	0.000 0	0.001 3	0.000 3
Cr	0.000 0	0.000 0	0.003 5	0.002 8	0.010 7	0.010 3	0.001 6	0.000 3	0.000 0	0.000 0	0.004 5
Fe <sup>3+</sup>	0.000 0	0.000 0	0.000 0	0.000 0	0.000 0	0.000 0	0.000 0	0.000 0	0.000 0	0.000 0	0.000 0
Fe <sup>2+</sup>	0.325 9	0.334 5	0.376 1	0.380 5	0.394 1	0.368 3	0.403 9	0.391 2	0.360 4	0.367 3	0.381 0
Mn	0.005 3	0.006 0	0.008 7	0.006 6	0.007 4	0.006 0	0.007 9	0.007 6	0.007 0	0.008 0	0.008 0
Mg	0.978 3	0.941 8	0.920 9	0.922 2	0.875 9	0.916 0	0.903 5	0.927 9	0.940 0	0.927 8	0.907 3
Ca	0.513 9	0.521 5	0.504 0	0.499 6	0.518 2	0.513 8	0.510 0	0.508 6	0.521 1	0.528 4	0.512 3
Na	0.008 3	0.020 2	0.019 1	0.011 0	0.021 3	0.014 7	0.010 4	0.008 6	0.013 4	0.009 8	0.018 2
K	0.002 0	0.005 3	0.003 1	0.001 9	0.004 7	0.004 1	0.003 6	0.003 7	0.003 6	0.006 6	0.004 2
Wo	28.27	29.01	27.98	27.72	28.98	28.57	28.06	27.83	28.61	28.98	28.45
En	53.81	52.39	51.13	51.17	48.98	50.94	49.72	50.77	51.61	50.88	50.39
Fs	17.92	18.60	20.88	21.11	22.04	20.48	22.22	21.40	19.78	20.14	21.16
Mg <sup>#</sup>	75.01	73.79	71.00	70.79	68.97	71.32	69.11	70.34	72.29	71.64	70.42
Cr <sup>#</sup>	0.00	0.00	3.43	3.15	7.10	9.02	1.54	0.32	0.00	0.00	5.98
											3.70

注: 分析测试单位为中国地质科学院地质研究所; 阳离子数的计算以6个氧原子数为基准; Mg<sup>#</sup>=100×Mg/[Mg+Fe<sup>2+</sup>], Cr<sup>#</sup>=100×Cr/[Cr+Al], Wo=100×Ca/[Ca+Mg+Fe<sup>2+</sup>], En=100×Mg/[Ca+Mg+Fe<sup>2+</sup>], Fs=100×Fe<sup>2+</sup>/[Ca+Mg+Fe<sup>2+</sup>]。

另外, 岩浆岩中 Si 与 Al 有互不相容的地球化学属性, 因此其 Si 和 Al 可作为确定母岩浆类型的标型元素(Le Bas, 1962; Leterrier *et al.*, 1982; Sun and Bertand, 1991; 孙传敏, 1994; Seyler and Bonatti, 1994; 邱家骥等, 1996)。具体而言, 单斜辉石中 Al<sup>IV</sup> 的含量取决于岩浆中硅的饱和度, 若岩浆中 Si 强烈不饱和, 造成单斜辉石在结晶时四面体位置 Si 不足, Al<sup>IV</sup> 进入四面体位置充填 Si 不足引起的空缺, 而四面体位置 Al<sup>IV</sup> 对 Si 替代所导致的电荷不平衡, 则要由 Al<sup>VI</sup>、Fe<sup>3+</sup> 和 Ti<sup>4+</sup> 进入到八面体位置来达到平衡(Campbell and Borley, 1974; Hode *et al.*, 1988; 寇彩化等, 2011)。由表 1 可知, 本次研究的绝大多数单斜辉石 Al<sup>IV</sup> 值为零, 指示单斜辉石的寄主岩石的母岩浆为 Si 饱和状态, 这与单斜辉石高 SiO<sub>2</sub> 而低 Al<sub>2</sub>O<sub>3</sub> 的特征一致。

综上所述, 单斜辉石的成分特征表明金车辉长岩的母岩浆应为硅饱和的拉斑玄武岩系列。

#### 4.2 温压估算及源区

依据 Putirka 等(2003)提出的辉石-熔体温压计计算了金车辉长岩单斜辉石形成的温度压力, 结果见表 3 和图 11a。金车辉长岩单斜辉石形成的温度较高, 介于 1 252~1 351℃, 压力较小, 为 1.31~2.25 GPa, 对应深度为 43.2~74.3 km。另外, 利用辉石成分等温线图解(图 11b)估计, 单斜辉石的形成温度变化范围约为 1 250~1 300℃, 与依据 Putirka 等(2003)估算的温度相当。

单斜辉石为金车辉长岩的主要造岩矿物, 而且是最早结晶的矿物, 所以单斜辉石的结晶温压可以代表金车辉长岩形成的温压条件。如前所述, 单斜辉石形成温度约为 1 250~1 350℃, 该温度与软流圈地

表2 金车辉长岩斜长石电子探针成分分析结果

 $w_B / \%$ 

Table 2 Chemical composition of plagioclase in the Jinche gabbro

样号	JC13-5	JC13-5	JC13-5	JC13-5	JC13-5	JC13-3	JC13-3	JC13-3	JC13-3	JC13-3	JC13-3
SiO <sub>2</sub>	68.35	68.02	66.30	68.15	67.81	67.18	67.33	67.68	66.76	67.50	66.75
TiO <sub>2</sub>	0.00	0.00	0.06	0.00	0.03	0.01	0.00	0.00	0.00	0.00	0.00
Al <sub>2</sub> O <sub>3</sub>	19.96	19.82	20.46	19.71	20.01	20.39	19.45	20.37	20.38	19.75	20.67
Cr <sub>2</sub> O <sub>3</sub>	0.00	0.03	0.04	0.02	0.02	0.02	0.00	0.00	0.00	0.00	0.03
FeO	0.10	0.01	0.75	0.10	0.11	0.09	0.10	0.02	0.03	0.00	0.03
MnO	0.00	0.04	0.05	0.00	0.00	0.01	0.00	0.01	0.00	0.00	0.00
MgO	0.00	0.00	0.76	0.00	0.00	0.07	0.10	0.00	0.01	0.00	0.00
CaO	0.56	0.70	0.97	0.45	0.52	1.68	1.61	1.40	1.60	1.48	1.45
Na <sub>2</sub> O	10.90	11.11	9.87	11.18	11.07	10.41	10.34	10.54	10.63	10.27	10.48
K <sub>2</sub> O	0.11	0.15	0.15	0.06	0.14	0.09	0.09	0.09	0.10	0.08	0.08
NiO	0.02	0.00	0.00	0.01	0.00	0.01	0.00	0.01	0.04	0.00	0.00
Total	100.01	99.88	99.42	99.69	99.70	99.96	99.02	100.12	99.53	99.09	99.49
Si	2.9842	2.9786	2.9551	2.9872	2.9745	2.9473	2.9785	2.9564	2.9407	2.9753	2.9374
Al	1.0273	1.0229	1.0750	1.0183	1.0346	1.0541	1.0138	1.0486	1.0578	1.0257	1.0718
Ca	0.0261	0.0326	0.0463	0.0213	0.0245	0.0791	0.0763	0.0653	0.0753	0.0700	0.0684
Na	0.9229	0.9434	0.8533	0.9502	0.9413	0.8853	0.8869	0.8927	0.9080	0.8774	0.8938
K	0.0063	0.0085	0.0086	0.0035	0.0079	0.0051	0.0049	0.0052	0.0055	0.0045	0.0043
Ba	0.0000	0.0000	0.0000	0.0000	0.0000	0.0000	0.0000	0.0000	0.0000	0.0000	0.0000
An	2.73	3.31	5.10	2.19	2.51	8.15	7.88	6.78	7.61	7.35	7.08
Ab	96.61	95.83	93.95	97.45	96.67	91.31	91.61	92.68	91.83	92.17	92.47
Or	0.66	0.86	0.95	0.36	0.82	0.53	0.51	0.54	0.56	0.47	0.45
样号	JC13-3	JC13-6	JC13-6	JC13-6							
SiO <sub>2</sub>	66.33	66.90	65.78	67.99	67.82	66.63	66.68	66.52	67.63	67.38	66.73
TiO <sub>2</sub>	0.00	0.00	0.00	0.01	0.00	0.00	0.00	0.00	0.00	0.00	0.00
Al <sub>2</sub> O <sub>3</sub>	20.46	19.67	20.69	19.47	19.96	20.24	20.36	20.76	20.00	19.74	20.35
Cr <sub>2</sub> O <sub>3</sub>	0.00	1.74	0.00	0.00	0.00	0.00	0.00	0.01	0.01	0.01	0.02
FeO	0.03	0.02	0.06	0.05	0.06	0.05	0.08	0.19	0.06	0.03	0.10
MnO	0.01	0.00	0.00	0.00	0.00	0.00	0.03	0.01	0.02	0.03	0.00
MgO	0.02	0.00	0.02	0.02	0.01	0.00	0.00	0.01	0.00	0.04	0.02
CaO	1.63	1.29	1.89	0.29	0.65	1.39	1.41	1.59	0.70	0.69	1.24
Na <sub>2</sub> O	10.34	10.25	10.40	11.44	11.00	10.59	10.54	10.57	11.06	11.20	10.67
K <sub>2</sub> O	0.09	0.14	0.11	0.11	0.11	0.16	0.12	0.10	0.19	0.18	0.13
NiO	0.01	0.00	0.00	0.00	0.02	0.01	0.01	0.01	0.00	0.00	0.00
Total	98.91	100.00	98.95	99.37	99.62	99.06	99.23	99.77	99.66	99.30	99.26
Si	2.9374	2.9738	2.9187	2.9908	2.9753	2.9468	2.9447	2.9279	2.9694	2.9721	2.9463
Al	1.0678	1.0303	1.0819	1.0096	1.0319	1.0548	1.0595	1.0769	1.0349	1.0261	1.0589
Ca	0.0771	0.0616	0.0896	0.0134	0.0304	0.0657	0.0665	0.0752	0.0330	0.0327	0.0586
Na	0.8880	0.8830	0.8943	0.9755	0.9359	0.9079	0.9026	0.9017	0.9411	.9579	0.9133
K	0.0050	0.0077	0.0061	0.0059	0.0063	0.0091	0.0069	0.0055	0.0104	0.0100	0.0074
Ba	0.0000	0.0000	0.0000	0.0000	0.0000	0.0000	0.0000	0.0000	0.0000	0.0000	0.0000
An	7.95	6.47	9.05	1.35	3.13	6.69	6.82	7.65	3.35	3.27	5.99
Ab	91.54	92.72	90.34	98.06	96.23	92.39	92.48	91.79	95.59	95.74	93.26
Or	0.51	0.81	0.61	0.59	0.64	0.92	0.70	0.56	1.05	1.00	0.76

注: 分析测试单位为中国地质科学院地质研究所; 阳离子数的计算以6个氧原子数为基准。

幔温度相当(1 280~1 350°C, Mckenzie and Bickle, 1988), 另外, 单斜辉石结晶时的压力为1.31~2.25 GPa, 对应的深度为43.2~74.3 km, 在该深度软流圈地幔可发生减压熔融(Mckenzie and Bickle, 1988)。因此, 金车辉长岩可能起源于软流圈地幔浅

部(约74 km), 是软流圈物质上涌并发生减压熔融的产物。

#### 4.3 构造意义及深部动力学过程

Nisbet等(1977)运用单斜辉石主要氧化物含量百分数构建了F<sub>1</sub>-F<sub>2</sub>因子判别图解, 用以判别岩浆

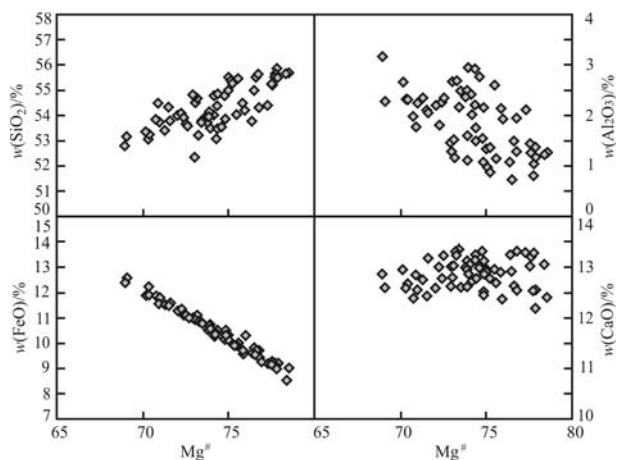


图 7 单斜辉石主要氧化物相关性图解

Fig. 7 Correlation between major oxides and  $Mg^{\#}$  in clinopyroxene

的构造环境。由图 12a 可知, 样品落入板内玄武岩和板内玄武岩 + 洋底玄武岩区内。另外, 根据 Leterrier 等(1982)建立的  $Ti - (Ca + Na)$  构造判别图

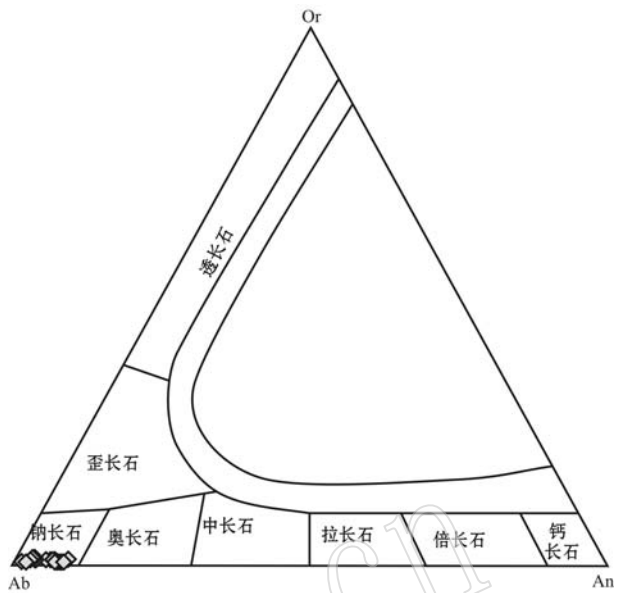
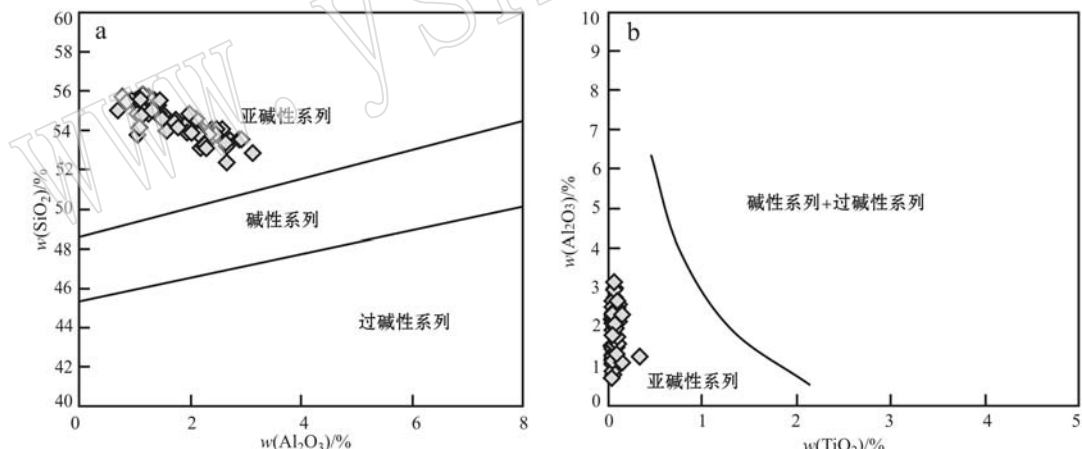


图 8 长石分类的 An-Ab-Or 成分三角图解(底图据

Smith and Brown, 1974)

Fig. 8 Classification of feldspar (after Smith and Brown, 1974)

图 9 单斜辉石  $SiO_2 - Al_2O_3$ (a) 和  $Al_2O_3 - TiO_2$ (b) 图解(底图据邱家骥等, 1996)Fig. 9 Diagrams of  $SiO_2 - Al_2O_3$ (a) and  $Al_2O_3 - TiO_2$ (b) of clinopyroxenes (after Qiu Jiaxiang et al., 1996)

解可知(图 12b), 本次研究的样品均落入板内拉斑玄武岩范围内。另外, 本次研究的金车辉长岩的单斜辉石与长界橄榄辉石岩的单斜辉石有着相似的矿物化学特征(寇彩化等, 2017), 作者之前的研究(寇彩化等, 2016)和作者未发表数据表明, 金车辉长岩与长界橄榄辉石岩皆具有板内拉斑玄武岩的全岩微量元素和同位素地球化学特征, 即, 金车辉长岩为典型

板内拉斑玄武岩。金车辉长岩和长界橄榄辉石岩分别形成于 730 Ma 和 700 Ma, 前人研究表明该阶段江南造山带西段处于裂谷背景下(王孝磊等, 2003; 舒良树, 2012; 寇彩化等, 2016), 因此, 初步推测金车辉长岩深部动力学机制可能与长界橄榄辉石岩相同, 皆与裂谷作用背景下软流圈物质上涌所引发的减压熔融有关。

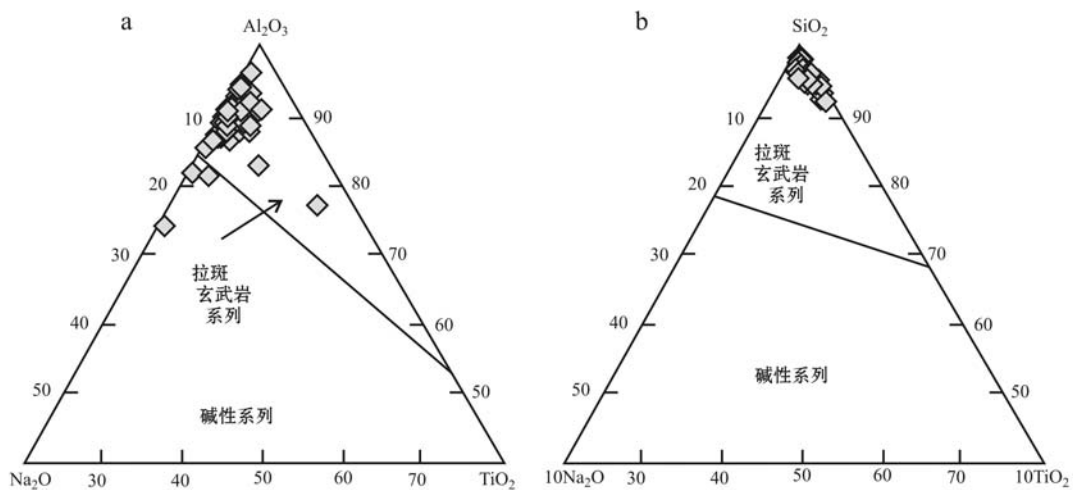
图 10 单斜辉石  $\text{Al}_2\text{O}_3 - \text{Na}_2\text{O} - \text{TiO}_2$ (a) 和  $\text{SiO}_2 - \text{Na}_2\text{O} - \text{TiO}_2$  图解(b)(底图据邱家骥等, 1996)

Fig. 10 Diagrams of  $\text{Al}_2\text{O}_3 - \text{Na}_2\text{O} - \text{TiO}_2$ (a) and  $\text{SiO}_2 - \text{Na}_2\text{O} - \text{TiO}_2$ (b) of clinopyroxenes  
(after Qiu Jiaxiang *et al.*, 1996)

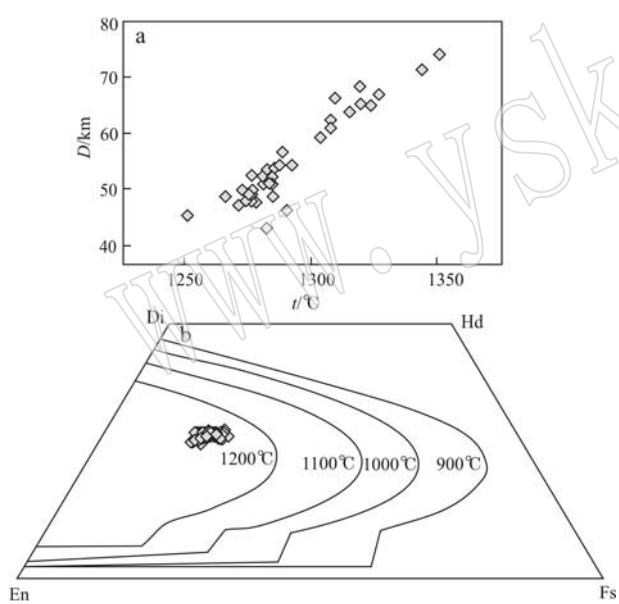


图 11 单斜辉石温度估算(b 底图据 Lindsley, 1983)

Fig. 11 The plot for pyroxene showing the equilibrium temperature (b after Lindsley, 1983)

## 5 结论

(1) 桂北龙胜地区金车辉长岩单斜辉石成分为  $\text{Wo}_{27-28}\text{En}_{47-57}\text{Fs}_{15-22}$ , 属于普通辉石。总体上表现出富镁和贫铁、钙、铝、钠、钛的特征; 斜长石主要为钠长石, 具有高硅、铝、钠以及低钙的特征。

(2) 桂北龙胜地区金车辉长岩母岩浆是 Si 饱和的拉斑玄武岩系列。

表 3 单斜辉石-熔体平衡温度、压力  
Table 3 Clinopyroxene-melt equilibrium temperatures and pressures

样号	$t/^\circ\text{C}$	$p/\text{GPa}$	$D/\text{km}$
JC13-5-1	1 291	1.40	46.2
JC13-5-2	1 283	1.31	43.23
JC13-1-1	1 308	1.88	62.04
JC13-1-2	1 285	1.58	52.14
JC13-1-3	1 288	1.65	54.45
JC13-1-4	1 316	1.94	64.02
JC13-1-5	1 320	2.07	68.31
JC13-1-6	1 308	1.85	61.05
JC13-1-7	1 327	2.03	66.99
JC13-1-8	1 351	2.25	74.25
JC13-1-9	1 320	1.98	65.34
JC13-1-10	1 286	1.63	53.79
JC13-1-11	1 304	1.80	59.4
JC13-1-12	1 272	1.43	47.19
JC13-1-13	1 344	2.17	71.61
JC13-1-14	1 324	1.97	65.01
JC13-1-15	1 277	1.45	47.85
JC13-1-16	1 279	1.45	47.85
JC13-1-17	1 277	1.51	49.83
JC13-1-18	1 285	1.48	48.84
JC13-1-19	1 285	1.54	50.82
JC13-1-20	1 275	1.46	48.18
JC13-1-21	1 284	1.55	51.15
JC13-1-22	1 293	1.65	54.45
JC13-3-1	1 310	2.01	66.33
JC13-3-2	1 289	1.72	56.76
JC13-3-3	1 277	1.59	52.47
JC13-3-4	1 252	1.38	45.54
JC13-3-5	1 277	1.49	49.17
JC13-3-6	1 276	1.49	49.17
JC13-3-7	1 283	1.62	53.46
JC13-3-8	1 282	1.54	50.82
JC13-3-9	1 281	1.59	52.47
JC13-3-10	1 267	1.48	48.84
JC13-3-11	1 273	1.51	49.83

注: 1 GPa 对应按 33 km 计算。

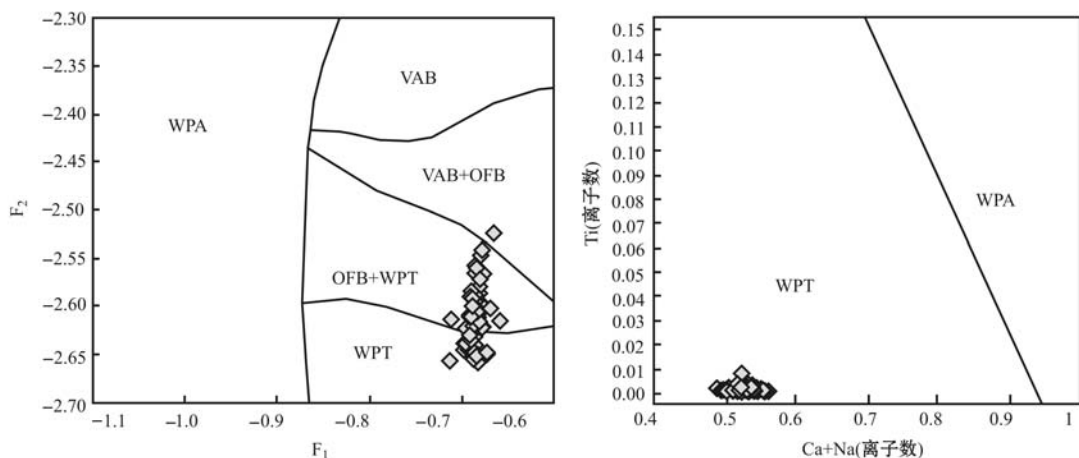


图 12 单斜辉石  $F_1 - F_2$  图解(a, 底图据 Nisbet and Pearce, 1977)和单斜辉石  $Ti - (Ca + Na)$  图解(b, 底图据 Leterrier *et al.*, 1982)

Fig. 12  $F_1 - F_2$  diagram (a, after Nisbet and Pearce, 1977) and  $Ti - (Ca + Na)$  diagram of clinopyroxene (b, after Leterrier *et al.*, 1982)

WPT—板内拉斑玄武岩; WPA—板内碱性玄武岩; VAB—火山弧玄武岩; OFB—洋底玄武岩

WPT—intraplate tholeiitic basalt; WPA—intraplate alkali basalt; VAB—volcanic arc basalt; OFB—ocean floor basalt

$$F_1 = -0.012(SiO_2) - 0.0807(TiO_2) + 0.0026(Al_2O_3) - 0.0012(FeO^T) - 0.0026(MnO) + 0.0087(MgO) + 0.0128(CaO) - 0.0419(Na_2O); F_2 = -0.0469(SiO_2) - 0.0818(TiO_2) - 0.0212(Al_2O_3) - 0.0041(FeO^T) - 0.1435(MnO) - 0.0029(MgO) + 0.0085(CaO) + 0.016(Na_2O)$$

(3) 估算所得单斜辉石形成的形成温度和压力分别为  $1250 \sim 1350^\circ C$  和  $1.31 \sim 2.25$  GPa, 对应深度为  $43.2 \sim 74.3$  km。

(4) 桂北龙胜地区金车辉长岩为典型的板内拉斑玄武岩, 起源于软流圈地幔, 其成因可能与裂谷背景下软流圈物质上涌发生的减压熔融作用有关。

**致谢** 感谢中国地质科学院地质研究所电子探针实验室戎合老师的指导和帮助, 感谢审稿人对论文提出的宝贵意见!

## References

- Campbell I H and Borley G D. 1974. The geochemistry of pyroxenes from the lower layered series of the Jimberlana intrusion, Western Australia[J]. Contributions to Mineralogy and Petrology, 47: 281~297.
- Faure M, Shu L S, Wang B, *et al.* 2009. Intracontinental subduction: a possible mechanism for the Early Palaeozoic Orogen of SE China [J]. Terra Nova, 21(5): 360~368.
- Gao Linzhi, Chen Jun, Ding Xiaozhong, *et al.* 2011. Zircon SHRIMP U-Pb dating of the tuff bed of Lengjiaxi and Banxi groups, north-

eastern Hunan: constraints on the Wuling Movement[J]. Geological Bulletin of China, 30: 1001~1008(in Chinese with English abstract).

Gao S, Ling W, Qiu Y, *et al.* 1999. Contrasting geochemical and Sm-Nd isotopic compositions of Archean metasediments from the Kongling high-grade terrain of the Yangtze craton: Evidence for cratonic evolution and redistribution of REE during crustal anatexis [J]. Geochimica et Cosmochimica Acta, 63: 2071~2088.

Ge Wenchun, Li Xianhua, Li Zhengxiang, *et al.* 2001. Mafic intrusion-sin Longsheng area: age and its geological implications[J]. Chinese Journal of Geology, 36(1): 112~118(in Chinese with English abstract).

Guo Lingzhi, Lu Huafu, Shi Yangshen, *et al.* 1996. On the meso-neoproterozoic Jiangnan island arc: its kinematics and dynamics[J]. Geological Journal of Universities, 2(1): 1~13(in Chinese with English abstract).

Guo Lingzhi, Shi Yangshen and Ma Ruishi. 1980. The geotectonic framework and crustal evolution of South China[A]. Scientific Paper on Geology for International Exchange[C]. Beijing: Geological Publishing House, 109~116(in Chinese with English abstract).

Hodge V J, Halenius U, Whitehouse M J, *et al.* 1988. Compositional variations (major and trace elements) of clinopyroxene and Ti-an-

- dradite from pyroxenite, ijolite and nepheline syenite, Alno Island, Sweden[J]. *Lithos*, 81: 55~77.
- Hu Shouxi and Ye Ying. 2006. Questions to “Cathaysia Old Land”, “CathaysiaBlock” and “United Yantze-Cathaysia Old Land” of South China Geological[J]. *Journal of China Universities*, 12(4): 432~439(in Chinese with English abstract).
- Kou Caihua, Liu Yanxue, Zhang Heng, et al. 2016. Geochronology and geochemistry of Neoproterozoic ultrabasic rocks from the Tongdao area in western Hunan Province, western segment of Jiangnan Orogen Belt, and constraints on their sources[J]. *Acta Petlogica et Mineralogia*, 35(6): 947~964(in Chinese with English abstract).
- Kou Caihua, Liu Yanxue, Zhang Heng, et al. 2017. Mineralogy of clinopyroxene of the Changjie olivine pyroxenolite in the Tongdao area in western Hunan Province and its geological significances [J]. *Geology Review*(in press, in Chinese with English abstract).
- Kou Caihua, Zhang Zhaochong, Liao Baoli, et al. 2011. Mineralogy of clinopyroxene of the Jianchuan picritic porphyrite in western Yunnan province and its geological significances[J]. *Acta Petlogica et Mineralogia*, 30: 449~462(in Chinese with English abstract).
- Le Bas M J. 1962. The role of aluminum in igneous clinopyroxenes with relation to their parentage[J]. *American Journal of Science*, 260: 267~288.
- Leterrier J, Maury R C, Thonon P, et al. 1982. Clinopyroxene composition as a method of identification of the magmatic affinities of paleo-volcanic seties[J]. *Earth and Planetary Science Letters*, 59: 139~154.
- Li X H. 1999. U-Pb zircon ages of granites from the southern margin of the Yangtze Block: timing of Neoproterozoic Jinning: Orogeny in SE China and implications for Rodinia Assembly[J]. *Precambrian Research*, 97(1): 43~57.
- Li X H, Li W X, Li Z X, et al. 2009. Amalgamation between the Yangtze and Cathaysia Blocks in South China: constraints from SHRIMP U-Pb zircon ages, geochemistry and Nd-Hf isotopes of the Shuangxiwu volcanic rocks[J]. *Precambrian Research*, 174(1): 117~128.
- Li X H, Li Z X, Zhou H W, et al. 2003. SHRIMP U-Pb zircon age, geochemistry and Nd isotope of the Guandaoshan pluton in SW Sichuan: Petrogenesis and tectonic significance [J]. *Science in China (Series D)*, 46: 74~83.
- Li X H, Zhu W G, Zhong H, et al. 2010. The Tongde Picritic Dikes in the Western Yangtze Block: Evidence for Ca. 800-Ma Mantle Plume Magmatism in South China during the Breakup of Rodinia [J]. *The Journal of Geology*, 118(5): 509~522.
- Li Z X, Li X H, Kinny P D, et al. 1999. The breakup of Rodinia: did it start with a mantle plume beneath South China? [J]. *Earth and Planetary Science Letters*, 173: 171~181.
- Li Z X, Li X H, Kinny P D, et al. 2003. Geochronology of Neoproterozoic syn-rift magmatism in the Yangtze Craton, South China and correlations with other continents: evidence for a mantle superplume that broke up Rodinia[J]. *Precambrian Research*, 122: 85~109.
- Li Z X, Zhang L H and Powell C M. 1995. South China in Rodinia: part of the missing link between Australia-East Antarctica and Laurentia? [J]. *Geology*, 23(5): 407~410.
- Lindsley D H. 1983. Pyroxene thermometry[J]. *American Mineralogist*, 68: 477~493.
- Mckenzie D and Bickle M J. 1988. The volume and composition of melt generated by extension of the lithosphere[J]. *Journal of Petrology*, 29: 625~679.
- Morimoto N, Fabries J, Ferguson K, et al. 1988. Nomenclature of pyroxenes[J]. *Mineralogy and Petrology*, 39 (1): 55~76.
- Nisbet E G and Pearce J A. 1977. Clinopyroxene composition in mafic lavas from different tectonic settings[J]. *Contributions to Mineralogy and Petrology*, 63(2): 149~160.
- Putirka K D, Mikaelian H, Ryerson F, et al. 2003. New clinopyroxene liquid thermobarometer for mafic, evolved, and volatile-bearing lava composition, with applications to lavas from Tibet and Snake River Plain, Idaho[J]. *American Mineralogist*, 88: 1542~1554.
- Qiu Jiaxiang and Liao Qun'an. 1996. Petrogenesis and Cpx mineral chemistry of Mineral Resources[J]. *Volcanology & Mineral Resources*, 17: 16~25 (in Chinese with English abstract).
- Seyler M and Bonatti E. 1994. Na, Al<sup>V</sup> and Al<sup>VI</sup> in clinopyroxenes of subcontinental and suboceanic ridge peridotites: a clue to different melting processes in the mantle? [J]. *Earth Planet Science Letter*, 122: 281~289.
- Shu Liangshu. 2012. An analysis of principal features of tectonic evolution in South China Block[J]. *Geological Bulletin of China*, 31(7): 1035~1053(in Chinese with English abstract).
- Shu L S, Faure M, Yu J H, et al. 2011. Geochronological and geochemical features of the Cathaysia block (South China): New evidence for the Neoproterozoic breakup of Rodinia[J]. *Precambrian Research*, 187: 263~276.
- Simith J V and Brown W L. 1974. Feldspar Minerals[M]. Germany:

- Springer-Ver-lag, 1~690.
- Streck M J. 2008. Mineral textures and zoning as evidence for open system processes[J]. *Reviews in Mineralogy and Geochemistry*, 69: 595~622.
- Sun Chuanmin. 1994. Genetic mineralogy of pyroxenes from Yanbian Proterozoic ophiolites (Sichuan, China), and its geotectonic implications[J]. *Journal of Mineralogy and Petrology*, 4: 1~15(in Chinese with English abstract).
- Sun C M and Bertrand J. 1991. Geochemistry of clinopyroxenes in plutonic and volcanic sequences from the Yanbian Proterozoic ophiolites (Sichuan Province, China): Petrogenetic and geotectonic implications[J]. *Schweiz Mineralogische Petroloische Mitteilungen*, 71: 243~259.
- Wang X L, Zhao G C, Zhou J C, et al. 2008. Geochronology and Hf isotopes of zircon from volcanic rocks of the Shuangqiaoshan Group, South China: Implications for the Neoproterozoic tectonic evolution of the eastern Jiangnan orogen[J]. *Gondwana Research*, 14: 355~367.
- Wang X L, Zhou J C, Griffin W L, et al. 2014. Geochemical zonation across a Neoproterozoic orogenic belt: Isotopic evidence from granitoids and metasedimentary rocks of the Jiangnan orogen, China[J]. *Precambrian Research*, 242: 154~171.
- Wang Xiaolei, Zhou Jincheng, Qiu Jiancheng, et al. 2003. Geochemistry of the Meso-Neoproterozoic volcanic-intrusive rocks from Hunan Province and its petrogenetic significances[J]. *Acta Petrologica Sinica*, 19(1): 49~60(in Chinese with English abstract).
- Wu R X, Zheng Y F, Wu Y B, et al. 2006. Reworking of juvenile crust: Element and isotope evidence from Neoproterozoic granodiorite in South China[J]. *Precambrian Research*, 146: 179~212.
- Xia Bin. 1984. A study on geochemical characteristic and emplaced style of two different ophiolites of later Proterozoic Xuefeng stage in the Longsheng regions, Guangxi Southeast China[J]. *Journal of Nanjing University (Natural Sciences)*, 3: 554~566(in Chinese with English abstract).
- Xue Huaimin, Ma Fang, Song Yongqin, et al. 2010. Geochronology and geochemistry of the Neoproterozoic granitoid association from eastern segment of the Jiangnanorogen, China: Constraints on the timing and process of amalgamation between the Yangtze and Cathaysia blocks[J]. *Acta Petrologica Sinica*, 26(11): 3215~3244(in Chinese with English abstract).
- Yan Q R, Hanson A D, Wang Z Q, et al. 2004. Neoproterozoic subduction and rifting on the northern margin of the Yangtze Plate, China: implications for Rodinia reconstruction[J]. *International Geology Review*, 46(9): 817~832.
- Yao J L, Shu L S, Santosh M, et al. 2013. Geochronology and Hf isotope of detrital zircons from Precambrian sequences in the eastern Jiangnan Orogen: Constraining the assembly of Yangtze and Cathaysia Blocks in South China[J]. *Journal of Asian Earth Sciences*, 74(2): 225~243.
- Yao J L, Shu L S, Santosh M, et al. 2014. Neoproterozoic arc-related mafic-ultramafic rocks and syn-collision granite from the western segment of the Jiangnan Orogen, South China: Constraints on the Neoproterozoic assembly of the Yangtze and Cathaysia Blocks[J]. *Precambrian Research*, 243: 39~62.
- Yu J H, Wang L J, O'Reilly, et al. 2009. A paleoproterozoic orogeny recorded in a long-lived cratonic remnant (Wuyishanterrane), eastern Cathaysia Block, China[J]. *Precambrian Research*, 174: 347~363.
- Zhang Chunhong, Fan Weiming, Wang Yuejun, et al. 2009. Geochronology and Geochemistry of the Neoproterozoic Mafic-Ultramafic Dykes in the Aikou Area, Western Hunan Province: Petrogenesis and Its Tectonic Implications[J]. *Geotectonica et Metallogenesis*, 33(2): 283~293(in Chinese with English abstract).
- Zhang S B, Zheng Y F, Zhao Z F, et al. 2008. Neoproterozoic anatexis of Archean lithosphere: Geochemical evidence from felsic to mafic intrusions at Xiaofeng in the Yangtze Gorge, South China[J]. *Precambrian Research*, 163: 210~238.
- Zhao G C and Cawood P A. 1999. Tectonothermal evolution of the Mayuan Assemblage in the Cathaysia Block: implications for Neoproterozoic collision-related assembly of the South China Craton [J]. *American Journal of Science*, 299(4): 309~339.
- Zheng Y F, Wu R X, Wu Y B, et al. 2008. Rift melting of juvenile arc ~ derived crust: Geochemical evidence from Neoproterozoic volcanic and granitic rocks in the Jiangnan Orogen, South China[J]. *Precambrian Research*, 163: 351~383.
- Zhong J, Chen Y J and Pirajno F. 2016. Geology, geochemistry and tectonic settings of the molybdenum deposits in South China: A review[J]. doi:10.1016/j.oregeorev.2016.04.012.
- Zhou J B, Li X H, Ge W C, et al. 2007. Age and origin of middle Neoproterozoic mafic magmatism in southern Yangtze Block and relevance to the break-up of Rodinia[J]. *Gondwana Research*, 12: 184~197.
- Zhou Jibin. 2006. Age and Origin of Neoproterozoic mafic magmatism in northern Guangxi-western Hunan: in response to the break-up of

- Rodinia? [D]. Guangzhou Institute of Geochemical, Chinese Academy of Geological Sciences (in Chinese with English abstract).
- Zhou J C, Wang X L and Qiu J S, et al. 2004. Geochemistry of Meso- and Neoproterozoic mafic-ultramafic rocks from northern Guangxi, China: Arc or plume magmatism? [J]. *Geochemical Journal*, 38: 139~152.
- Zhou J C, Wang X L and Qiu J S. 2009. Geochronology of Neoproterozoic mafic rocks and sandstones from northeastern Guizhou, South China: Coeval arc magmatism and sedimentation[J]. *Precambrian Research*, 170: 27~42.
- 高林志, 陈 峻, 丁孝忠, 等. 2011. 湘东北岳阳地区冷家溪群和板溪群凝灰岩 SHRIMP 锆石 U-Pb 年龄——对武陵运动的制约[J]. *地质通报*, 30: 1 001~1 008.
- 葛文春, 李献华, 李正祥, 等. 2001. 龙胜地区镁铁质侵入体: 年龄及其地质意义[J]. *地质科学*, 36(1): 112~118.
- 郭令智, 卢华夏, 施央申, 等. 1996. 江南中、新元古代岛弧的运动学和动力学[J]. *高校地质学报*, 2(1): 1~13.
- 郭令智, 施央申, 马瑞士. 1980. 华南大地构造格架和地壳演化[A]. 26届国际地质大会论文集(1)[C]. 北京: 地质出版社, 109~116.
- 胡受奚, 叶 瑛. 2006. 对“华夏古陆”、“华夏地块”及“扬子-华夏古陆统一体”等观点的质疑[J]. *高校地质学报*, 12(4): 432~439.
- 寇彩化, 刘燕学, 张 恒, 等. 2016. 江南造山带西段湘西通道地区新元古代超基性岩体年代学和岩石地球化学研究及其对源区的约束[J]. *岩石矿物学杂志*, 35(6): 947~964.
- 寇彩化, 刘燕学, 张 恒, 等. 2017. 湘西通道地区长界橄榄辉石岩中单斜辉石矿物学特征及其地质意义[J]. *地质论评(待刊)*.
- 寇彩化, 张招崇, 廖宝丽, 等. 2011. 滇西剑川苦橄玢岩中单斜辉石的矿物学特征及其地质意义[J]. *岩石矿物学杂志*, 30: 449~462.
- 邱家骥, 廖群安. 1996. 浙闽新生代玄武岩的岩石成因学与 Cpx 矿物化学[J]. *火山地质与矿产*, 17: 16~25.
- 舒良树. 2012. 华南构造演化的基本特征[J]. *地质通报*, 31(7): 1 035~1 053.
- 孙传敏. 1994. 四川盐边元古代蛇绿岩中辉石的成因矿物学及其大地构造意义[J]. *矿物岩石*, 14: 1~15.
- 王孝磊, 周金城, 邱检生, 等. 2003. 湖南-中-新元古代火山-侵入岩地球化学及成因意义[J]. *岩石学报*, 19(1): 49~60.
- 夏 斌. 1984. 广西龙胜元古代二种不同成因蛇绿岩岩石地球化学及侵位方式研究[J]. *南京大学学报*, 3: 554~566.
- 薛怀民, 马 芳, 宋永勤, 等. 2010. 江南造山带东段新元古代花岗岩组合的年代学和地球化学: 对扬子与华夏地块拼合时间与过程的约束[J]. *岩石学报*, 26(11): 3 215~3 244.
- 张春红, 范蔚茗, 王岳军, 等. 2009. 湘西隘口新元古代基性-超基性岩墙年代学化学特征: 岩石成因及其构造意义[J]. *大地构造与成矿学*, 33(2): 283~293.
- 周继彬. 2006. 桂北-湘西新元古代镁铁质岩的形成时代和成因——对 Rodinia 超大陆裂解的响应[D]. 中国科学院广州地球化学研究所.